JOURNAL OF MATERIALS SCIENCE 30 (1995) 2201–2214

Morphology of melt crystallized polypropylene in the presence of polyimide fibres*

T. E. SUKHANOVA, F. LEDNICKÝ§, J. URBAN§, Y. G. BAKLAGINA, G. M. MIKHAILOV, V. V. KUDRYAVTSEV
Institute of Macromolecular Compounds of Russian Academy of Sciences, Bolshoi pr. 31, 199004 Saint-Petersburg, Russia and §Institute of Macromolecular Chemistry, Academy of Sciences of the Czech Republic, Heyrovský Sq. 2, 16206 Prague 6, Czech Republic

Hot stage optical and scanning electron microscopy were used to study isothermal crystallization of isotactic polypropylene (iPP) in the presence of polyimide (PI) fibres. Under the same crystallization conditions, the occurrence of transcrystallization depends on the type of fibre used. The transcrystalline interphase has a composed structure, with a characteristic layer adjacent to the fibre surface. The layer is about 1 μm thick and has a crosshatched lamellar morphology. At the interface between iPP and the PI fibre which causes transcrystallization, the nuclei from which the transcrystalline zone grows is observed. The nuclei consist of sheaves of closely packed parallel needleshaped lamellae of uniform thickness. The transcrystallization phenomenon can be explained by the epitaxial crystallization of iPP matrix on the surface fragments (domains) formed by extended chains of PI fibres. Different abilities of PI fibres to induce transcrystallization are associated with the superficial morphology of the fibres.

1. Introduction

Thermoplastic polymers like isotactic polypropylene (iPP) are usually reinforced with various types of polymer or glass fibres to form composites with improved properties [1–5]. It is well established that these fibre reinforced composites have higher stiffness, tensile strength and higher modulus than the neat iPP [1–7]. Extensive investigation showed that the incorporation of fibres may result in changes in the morphology and crystallinity of the interphase region [1, 3, 8, 9], and that some polymer and organic fibres have an ability to nucleate crystallization along the fibre surface with a sufficiently high density of nuclei [8–12]. This results in the growth of matrix spherulites, only in the radial direction, and a columnar crystalline layer arises around the fibre. This phenomenon called transcrystallization [13] is a subject of a large number of investigations, as it has significant influence on the performance of fibre reinforced thermoplastic composites. Improvements in the mechanical [3, 4–7, 11, 12, 14], transverse [15, 16] and impact properties [17] was observed in cases where the reinforcing fibres, acting as nucleating agents, caused transcrystallization. It was suggested that the transcrystallinity may result in a higher adhesion between the fibres and matrix [18–20] and lead to a synergism of mechanical properties. However, the literature reports on the decrease in fibre–matrix bond strength due to transcrystallinity [19–21] or on the absence of improvements in interfacial adhesion [22, 23].

Transcrystallization was observed for a variety of polymer melt–substrate pairs and crystallization conditions [1–26]. It occurs in many semicrystalline polymers (nylon 6, nylon 66, PE, PEEK, iPP) crystallized in contact with thermoplastic fibres, high modulus carbon fibres, some organic and copper fibres [11, 12 and references therein]. A large number of factors were studied with respect to the ability to nucleate transcrystalline growth, such as chemical composition of the fibre surface, crystalline structure and surface energy of the substrate, temperature gradients along the fibre and evolution of volatile products from the substrate. However, none of the investigated factors was found to play a decisive role in the transcrystallinity. Moreover, the morphology of the interphase and the nucleation process of the transcrystalline zone have not yet been quite cleared up.

The studies referred to, however, showed the irrelevance of the following factors for the effect of strong nucleation [27]

1. similarity of the chemical structure of substrate and deposited polymers;
2. similarity of crystallographic unit cell geometries;
3. close match of crystal lattice parameters of the polymer pair; and
4. similarity of chain conformation.

* Presented in part at the 28th Europhysics Conference on Macromolecular Physics, "Transitions in Oligomer and Polymer Systems" 27 September–1 October 1993, Ulm, Germany.

0022–2461

Thomason and van Rooyen found that the transcrystalline interphase depends on the type of fibre used and on crystallization conditions during quiescent crystallization [11]. They investigated the phenomenon of transcrystallization for a large number of polymer fibres in contact with iPP. From the experiments with fibres pulled out of the supercooled polymer melt [12], they also proposed that transcrystallization has a stress induced nature due to the stresses caused by cooling of two materials with a large difference in their thermal expansion coefficients (TEC). However, the full explanation of the transcrystallization involves not only a stress induced nature, but also the level of fibre–melt interaction [12]. It is assumed that stress or shear induced crystallization is related to transcrystallization, because these phenomena cannot be distinguished using polarized light microscopy.

Devaux and Chabert [28, 29] offered another view on these phenomena in their study of shear induced non-isothermal crystallization of iPP in the presence of glass and jute fibres. They concluded that the application of shear stresses at the iPP–glass fibre interface promotes the growth of a crystalline superstructure similar to transcrystallization. This particular interphase may consist of α phases or α and β phases simultaneously, according to the condition of crystallization [29]. It was proposed that the transcrystalline-like superstructure is probably due to the multiplication of macromolecular entanglements adjacent to the fibres, while transcrystallization is linked to the superficial characteristics of the fibres and nucleation occurs actually on the fibre surface.

Varga and Karger-Kocsis found in their recent work [30] that the transcrystalline-like superstructures, produced by pulling a glass fibre from iPP melt, are caused by α row nucleation (selfnucleation) developed by shearing the melt instead of transcrystalline layers (heterogeneous nucleation). They pointed out that it is necessary to make a clear distinction between cylindritic (transcrystalline-like) crystallization and transcrystallization itself. They observed the superstructures which consisted of α row-nuclei and β cylindrites around fibres and supposed that this feature is related to some kind of epitaxial growth.

Only little attention has been devoted to the crystalline structure of the matrix in the vicinity of the surface of fibres embedded in the melt. The crystallization of nylon 6 matrix from the melt filled with para aromatic polyamide (PA) fibres was studied by Oono *et al.* using microbeam X-ray diffraction [31]. It was shown that crystallization is induced on the surface of microfibrils of rigid PA and, on the basis of aggregation structure, that the transcrystalline zone consists of two regions: an interfacial zone about 3 μm thick adjacent to the fibre surface, and an intermediate zone which extends to the matrix.

Epitaxy was used to explain the surface induced transcrystalline interphase in composites with aramid [32] and pitch based carbon fibres [32–34], whereas in polyacrylonitrile (PAN) based carbon fibres and glass fibre systems, in which transcrystallization occurs only under special circumstances, this phenomenon was attributed to the thermal conductivity mismatch [32].

Despite extensive investigations of transcrystallization, neither requirements for the character of foreign surfaces to be active in heterogeneous nucleation nor the mechanism of the process are fully understood yet, and thus transcrystallization remains a phenomenon of general interest.

The aim of the present work is to contribute to the understanding of how the presence of fibres influences the crystallization of thermoplastic matrix and to propose a mechanism of transcrystalline nuclei generation. Isothermal crystallization of iPP filled with several aromatic polyimide fibres (PI), the chemical structure of which is similar, but with a varied morphology and crystalline structure have been investigated. These fibres have several valuable properties, such as high heat resistance and heat stability, maintaining good mechanical properties [35]. The high modulus and tensile strength of some PI fibres make them useable as reinforcing fibres in composite materials. There are many examples in the literature showing the influence of aramid fibres, such as Kevlar, Twaron, high modulus and high strength carbon fibres, nylon 6, nylon 66, glass and other fibres, on the crystallization of iPP [1, 6–9, 11, 12, 36]. All these fibres were industrial products and there was only minor information about their origin and treatment. On the other hand, the fibres reported in this article were of known origin and without any additional surface treatment.

In the studies of transcrystallization, hot stage optical microscopy is most frequently used [1, 3, 6–13, 17–26, 28–32], sometimes in combination with differential scanning calorimetry [14, 28, 29], X-ray diffraction [31, 37] and dynamic mechanical spectroscopy [38]. In this study, scanning electron microscopy was engaged to evaluate the fibre surface topography, to disclose the interface morphology and to observe the nuclei from which the transcrystalline zone grows.

2. Experimental procedure

2.1. Materials

Commercial isotactic polypropylene (Mosten 58.412 CHZ Litvínov, Czech Republic) of melt flow index 3–4, 98% isotacticity and molecular weight–molecular numbers M_w/M_n, equal to nine was used.

Polyimide fibres PI-1 (Arimid T, Dorkhimzavod, Russia) made of poly(pyromellitic dianhydride-*alt*-4,4′-diaminodiphenyl ether) with diameter about 15 μm were used. The other types of polyimide fibres (PI-2, PI-3 and PI-4) were obtained by a two-stage method [35]. They were derived from pyromellitic dianhydride or 4,4′-oxybis(phthalic anhydride) and diamines 4,4″-diamino-p-terphenyl, p-phenylenediamine or 2,5-bis(4-aminophenyl)-pyrimidine.

In the first stage, poly(amic acid) fibres were prepared from 12% solutions of prepolymers in *N*,*N*-dimethylacetamide by the wet spinning process in a coagulation bath (1 : 1 aqueous dimethylacetamide). In the second stage, the polyimide fibres were obtained by thermal imidization of poly(amic acid) fibres by heating up to 400 °C. The obtained fibres had different diameters: 54.0 (PI-2), 51.0 (PI-3) and 48.3 μm (PI-4).

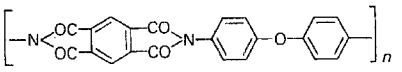
PI-1

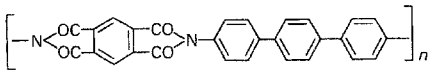
PI-2

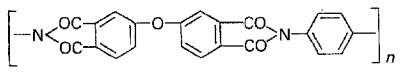
PI-3

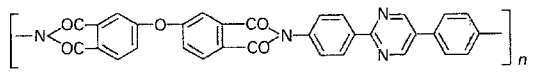
PI-4

2.2. Sample preparation for optical observation

Fibres were sandwiched between two thin plates of iPP (30–40 μm) and after annealing at ~ 200 °C in a nitrogen atmosphere for about 5 min, the plates were pressed together. The obtained samples were ~30–40 μm thick.

Optical investigations were carried out in the course of crystallization with the aid of a Zeiss–Opton microscope, Photomikroskop III. Samples were pressed between glass slides. Isothermal crystallization was carried out on a Mettler microscope heating stage, model FP5/FP52. In order to eliminate the influence of thermal history on crystallization, every sample was annealed at 200 °C for 5 min and quickly cooled (during 3–4 min) to the crystallization temperature, 124–135 °C.

Samples of fibre reinforced composites for simple mechanical tests were prepared in a special metallic form. Several plates of iPP 0.3–0.4 mm thick, obtained from melted granules, with 10–30 parallel fibres between them, were heated to 210–220 °C for 4–5 min in a nitrogen atmosphere to ensure complete melting, yet minimizing any thermal degradation of iPP. After that, the isothermal crystallization was carried out in a temperature controlled oven at 135 °C for 25 min. Calibration, using phenacetin crystals as a standard (melting point, 135 °C) showed that the temperature of the heater was accurate to ± 0.2 °C. Then, the samples were cooled in quiescent air under room conditions. Composite samples thus obtained were 2–3 mm thick, the other dimensions being 8 and 24 mm.

Cut surfaces were prepared by cutting these samples on a microtome in transverse and longitudinal directions and then investigated by electron microscopical methods (EM).

2.3. Sample preparation for EM observation

Before EM observation, samples were etched by the permanganic etching method recommended by Olley and Basset [39] and used by Rybnikář [40–42] for the observation of fine details of spherulitic structures in iPP (agent I, 85% H_3PO_4 with 1.3% $KMnO_4$; or agent II, 96% H_2SO_4 and 85% H_3PO_4, 1:1 by volume, with 1.3% $KMnO_4$ were used). This etching procedure removes preferentially the amorphous phase of the polymer, while the lamellar structure of the spherulites remains intact and can be clearly observed.

Finally, etched surfaces were sputter coated with a very thin layer of gold (models 07 120 or SCD 050 ion sputtering devices, Balzers, Switzerland) for the scanning electron microscopy (JSM-4600, Jeol).

X-ray diffraction analysis of PI fibres was carried out using a Dron-2 diffractometer and an RKV-86 A camera with CuK_α radiation and Ni filter.

3. Results and discussion

3.1. Nucleating ability of PI fibres

Optical microscopy in polarized light shows the differences in neat iPP, Fig. 1a, which crystallized in the form of spherulites, and in the presence of various PI fibres, Fig. 1b–e. Optical micrographs of the early stages of crystallization (spherulites surrounded by the melt, Figs 1 and 2) show that PI-1 fibres, Fig. 1b, have no effect on the morphology of iPP. Only spherulitic morphology can be observed in this case, with an enhanced number of spherulites grown near the fibres. No crystalline entities exist in longer parts of fibres at the early stages of the crystallization process, nor do the ends of fibres cause any transcrystallinity. PI-1 fibres appear to be inactive according to the classification in [24], similarly to, for example, glass fibres and high strength and intermediate modulus carbon fibres [11].

High modulus fibre PI-4 can serve as an example of the fibre which induced transcrystallization, Fig. 1e. It appears like a white band around the fibres, located along their whole length. These "columnar" transcrystalline regions consist of densely packed, radially orientated crystalline lamellae, which grow in the direction of the fibre radius because of high concentration of the nuclei on the fibre surfaces. The transcrystallized regions extend to ~ 80 μm from the fibre surfaces, corresponding to the maximum radius of bulk spherulites grown isothermally at 135 °C for 25 min. This means that the rates of growth of the transcrystalline region and spherulites are equal. The equal growth rates of the transcrystalline zone and those of matrix spherulites were also reported for various systems [11]. According to the criteria in reference [24], PI-4 is an active fibre for iPP matrix.

Other selected PI fibres, PI-2 and PI-3 (Fig. 1c and d, respectively), also induce transcrystallization, but the nucleation density is lower. These fibres are moderately active [24].

The occurrence of transcrystallization was shown to depend on several parameters, among them is the molecular weight of the polymer [11, 12]. When the molecular weight is increased, the temperature limit, below which transcrystallization occurs, increases (from 138 °C for Shell S6100 iPP with $M_w = 270\,000$ and $M_n = 37\,000$, to 145 °C for HY6100 iPP with $M_w = 380\,000$ and $M_n = 66\,500$). Thus, decreasing the molecular weight due to a longer heating time or heating above 250 °C causes a decrease in the temperature limit of transcrystallization phenomenon and a reduction in the number of spherulites in the matrix. Decreasing the molecular weight can also be caused

by the second heating of the samples [14]. The present results, on the contrary, show that the second annealing at 220 °C for 15 min, followed by cooling to the crystallization temperature of 130 °C at a rate of 3 K min^{-1}, does not change the nucleation ability of PI-4 fibres. The fibres induce transcrystallization with the same rate, only the number of spherulites in the field of view is substantially decreased, Fig. 2a–d. Moreover, spherulites distant from the fibre change their type: after the first heating, Fig. 2a,b, α mixed spherulites can be seen; and after the second heating, the spherulites are much closer to pure α type [8]. A similar result was obtained by Lee and Porter [15] for PEEK–carbon fibre composites. These data contradict the finding of Chatterjee and Price [24], who claim that in the melt crystallization of polymers there exists a fixed number of nucleating sites on the substrate surface and in the bulk at a given temperature.

When the degradation of iPP occurs, the number of active sites in the bulk and on the substrate surface must reduce and the transcrystallization should be depressed. However, the present results are not in agreement with the concept of a fixed number of nuclei as mentioned above. It may be suggested that the surface's nucleating ability does not depend strongly on the molecular weight of the matrix polymer, and the mechanisms of nuclei generation at the interface and in the bulk can be different.

3.2. Structure of PI fibres

SEM analysis of the surface morphology of isolated PI fibres shows that all the PI fibres studied have macroheterogeneous structure with differences in porosity, shape, dimensions of fibrils, size of fibrillar aggregates, Fig. 3a–h, and surface topography, Fig. 3b, d, f, h. It follows from the hot stage optical microscopy data, Figs 1 and 2, that PI-4 fibres, Fig. 3g, h induce a high density transcrystallization, PI-2 and PI-3 fibres, Fig. 3c–f, a moderate density transcrystallization and fibres PI-1, Fig. 3a, b, induce no transcrystalline growth at all. After permanganic etching (agent I), very marked differences between the morphologies of PI fibres come into particular prominence, Fig. 4a–c. For comparison, micrographs of the etched surfaces were obtained at the same magnification after etching of PI-1–PI-4 fibres for 2 min. The PI-1 fibre has a smooth relief without fibrillar structure (Fig. 4a); while the PI-4 fibre exhibits a well developed fibrillar structure, which becomes more visible when the etching time is increased, Fig. 4b, c. On the surface of the PI-4 fibre, fibrillar parts and less ordered parts without fibrillar structure exist simultaneously, Fig. 4b, c. PI-2 and PI-3 fibres also have fibrillar and smooth parts on the surface. Therefore, it may be concluded that the topography of the fibre surface on this "macrolevel" for fibres which induce transcrystallization is complex, and all these fibres have a rough surface relief.

The X-ray diffraction patterns of PI fibres, Fig. 5a–d, exhibit reflections related to periodicity along the polymer chains. The existence of clear meridional reflections for PI-2, PI-3 and PI-4 fibre demonstrate regular arrangement of the polymer chains

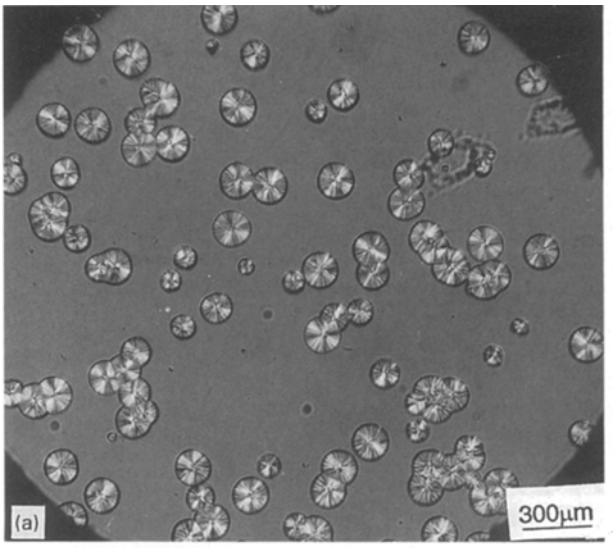

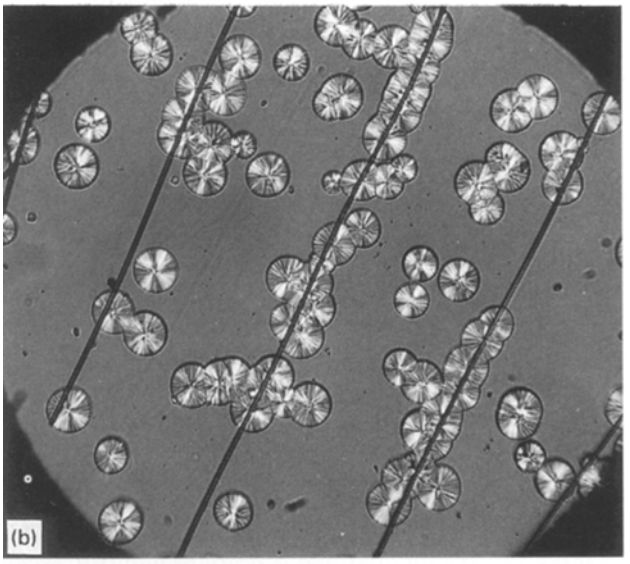

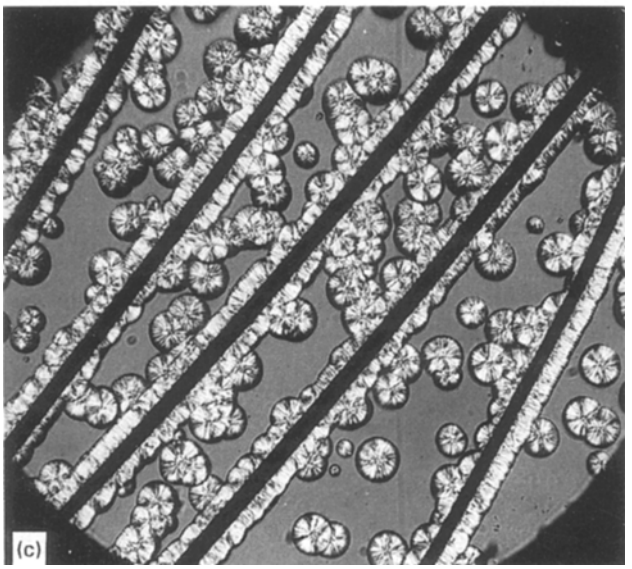

Figure 1 Optical micrographs of partially crystallized samples in the course of isothermal crystallization at 135 °C after 25 min: (a) neat iPP, (b) iPP filled with PI-1, (c) PI-2, (d) PI-3 and (e) PI-4 fibres.

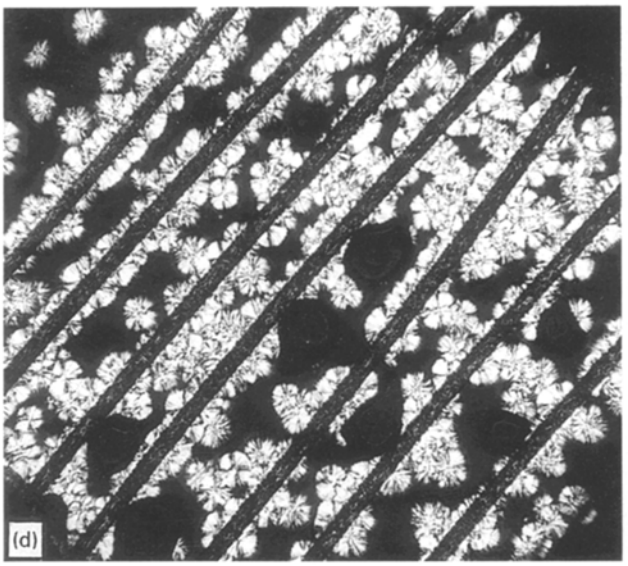

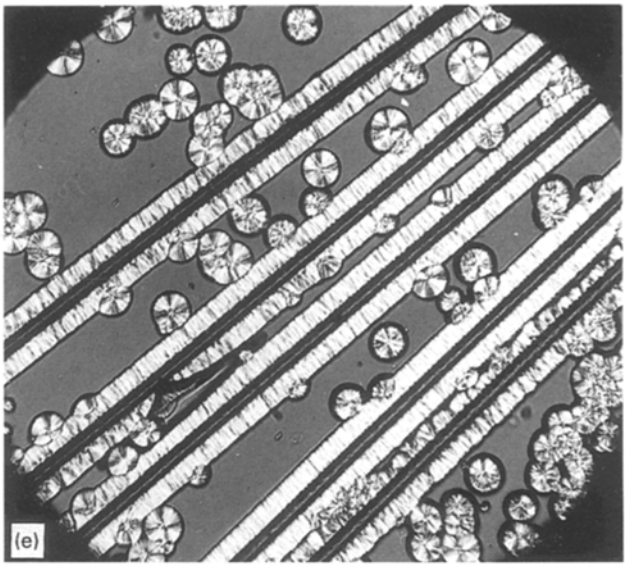

Figure 1 (continued)

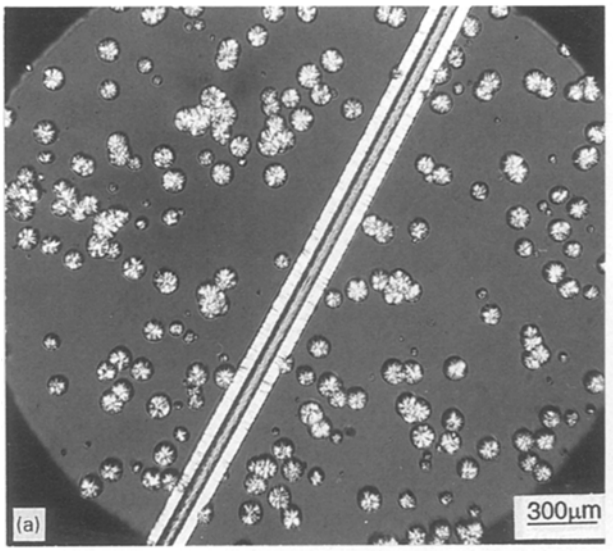

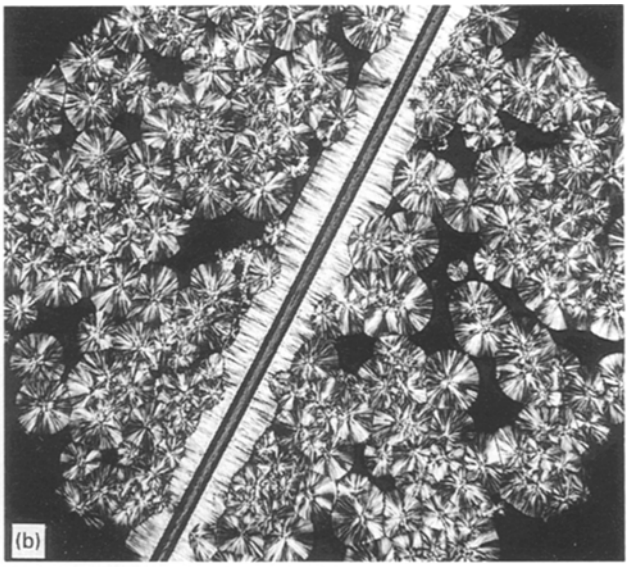

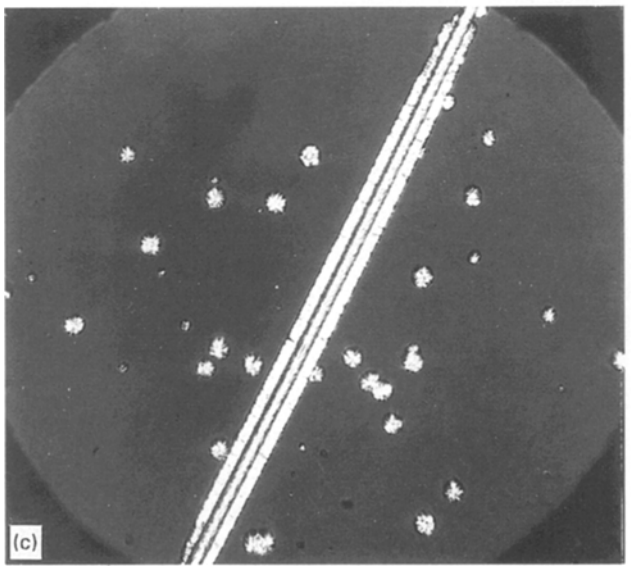

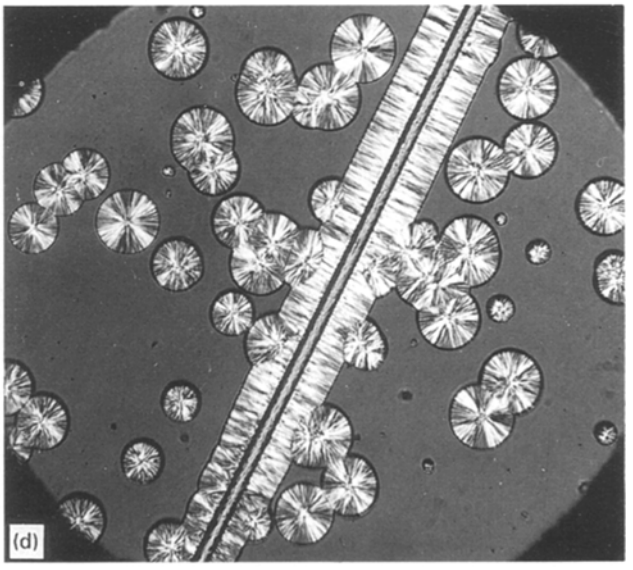

Figure 2 Optical micrographs of partially crystallized samples in the course of isothermal crystallization of iPP with a single PI-4 fibre embedded. First melting at 220 °C during 15 min, followed by crystallization at 130 °C during (a) 5 min or (b) 15 min; (c) after the second melting and crystallization cycle in the same conditions 5 min or (d) 15 min.

along the fibre axis. A comparison of unit cell dimensions between the iPP and PI fibres used is listed in Table I.

It is known that α spherulites of iPP have monoclinic crystalline form and three-fold helical conformation, with a 0.65 nm repeat distance [27]. The crystal structure of the PI-2 fibre is orthorhombic with the *c*-axis oriented parallel to the fibre axis. Macromolecules of PI-2 have rod-like conformations. Planar pyromellitic and phenylene moieties are arranged in parallel planes. The mutual packing of these fragments leads to the formation of densely packed layers with the greatest contribution to the energy of the lattice provided by the van der Waals' interactions [44]. PI-3 and PI-4 have an oxygen atom in the dianhydride moieties and the result is the rotation of polymer chains around it, but the conformation of chains in PI-3 and PI-4 is also extended. According to [45], these PI represent a layered structure. It was supposed [45] that these PI fibres have domain structure with extended parallel chains and a high degree of chain orientation. On the other hand, PI-1 fibres are a much more disordered mesomorphic system and crystallize ery poorly. The small ordered domains (about 4 nm [43]) arise only after annealing at 500–550 °C.

Analysis of the equatorial regions of diffractograms indicates that the order of the intermolecular packing is lower in the transversal direction in PI-1 than in other PI fibres. The angle of disordering along the chain axis for PI-1 is about 60° and for PI-4 about 20–30° [44]. Thus, PI-1 has a mesomorphic structure, the other fibres are crystalline with the orientation degree increasing in the sequence PI-4, PI-3, PI-2.

3.3. Influence of fibre surface on matrix nucleation

The etched transversal Fig. 6a–d, and longitudinal, Fig. 6e, f, cutting surfaces of iPP composites with PI-1 fibres (agent II) show that the matrix spherulites grow around these fibres and their nuclei usually arise inside the matrix near the PI-1 fibre surface, Fig. 6b. On the transverse cutting surfaces one or two large spherulites developed around the fibre can be observed. The lamellae of these spherulites grow round the PI-1 fibre surface.

The spherulites may arise also from contact points between fibres or from regions in which the fibres are almost in contact, Fig. 6c, as a result of local shearing. Fig. 6d shows the matrix spherulite which finished its growth on the PI-1 fibre surface.

Longitudinal sections of the composite with PI-1 fibres, Fig. 6e, f, reveal a series of radial growth patterns originating from well separated nucleation sites within the matrix. There is no sign of other competing nucleation events in this case. Along the fibre surface, the spherulites are more or less disturbed unlike the bulk matrix and the morphology seems to be the same as without fibres. In Fig. 6f the hollow nest of the absent fibre is clearly visible. One can see several spherulites with a distance of 10–40 μm between their centres. At high magnifications, Fig. 7a, b, the lamellar structure at the interface looks like the structure in the matrix. Thus, the general features of the iPP morphology are the same at the interface as in the matrix in the case of inactive PI-1 fibres.

Closer inspection reveals a very marked difference between the interface morphology in the case of coexisting PI-4 fibres, as compared with PI-1 fibres.

One can see the radial lamellar growth, Fig. 8a, which arises from the fibre surface, Fig. 8b, and the fibre surface relief is replicated by the iPP matrix. There appears to be a very good wettability of PI fibres by the polymer melt. The etchant removed a thin layer of iPP leaving the ends of the PI-4 fibres protruding about 3 μm from the matrix.

The distribution of the nucleating sites along the fibre surface is not homogeneous. Fig. 8c shows the spherulite growth from the concave fragment of the PI-4 surface, while the others part of the surface have no nucleating sites.

An investigation of the interfacial zone of the rich variety of PI-4 fibres in the iPP matrix showed that thin sheathes, 1–2 μm thick, around the fibres exist, with the morphology slightly different from that of the transcrystalline zone. This means that the transcrystalline zone has a composed structure. This composed structure can be seen also on the longitudinal sections, Fig. 8d–f. It should be pointed out that in the case of PI-4 fibres the hollow nest of the absent fibre, Fig. 8d, does not have visible spherulites. The comparison of

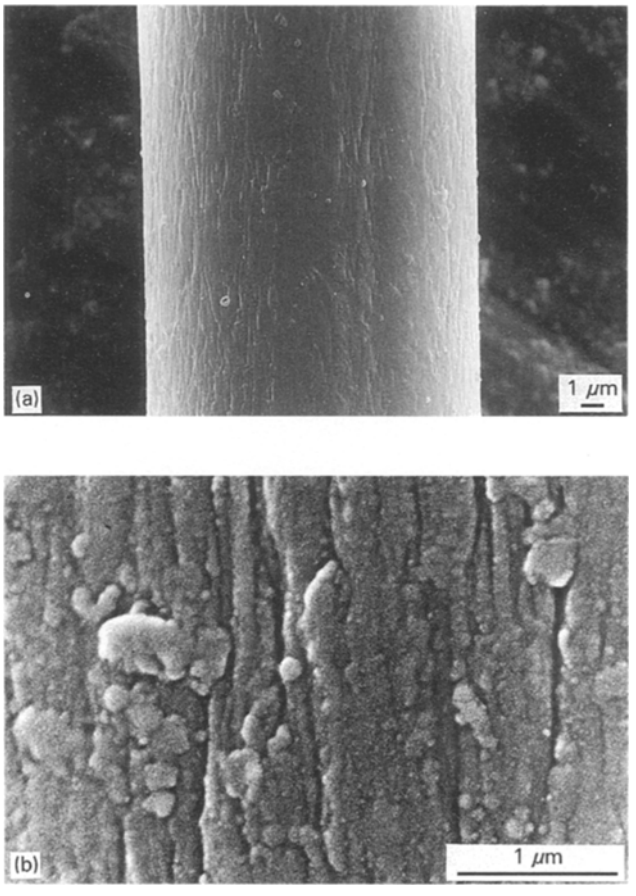

Figure 3 SEM micrographs of PI fibres: (a,b) PI-1, (c,d) PI-2, (e,f) PI-3 and (g,h) PI-4. General view of fibres (a,c,e,g); surface details (b,d,f,h).

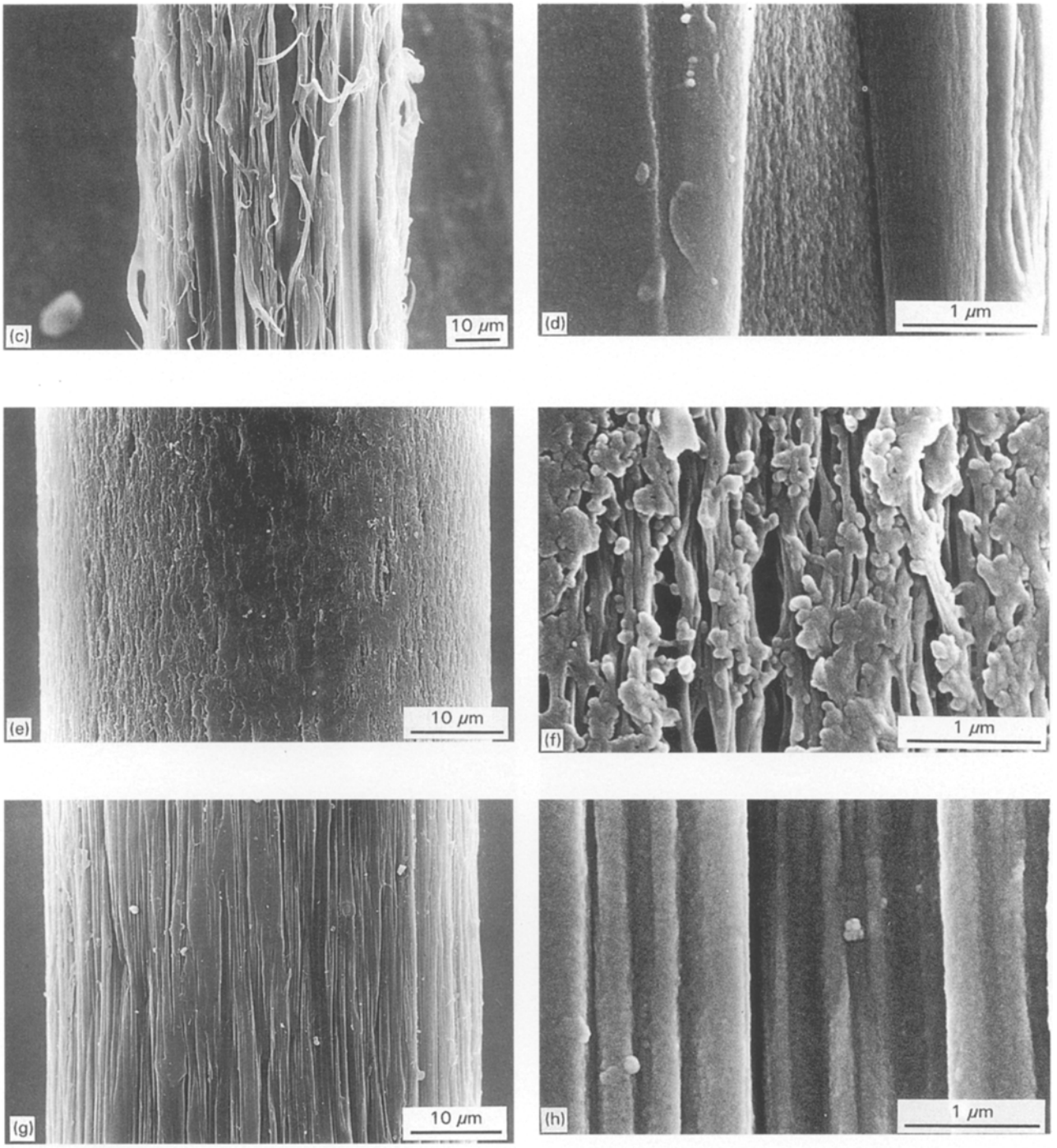

Figure 3 (continued).

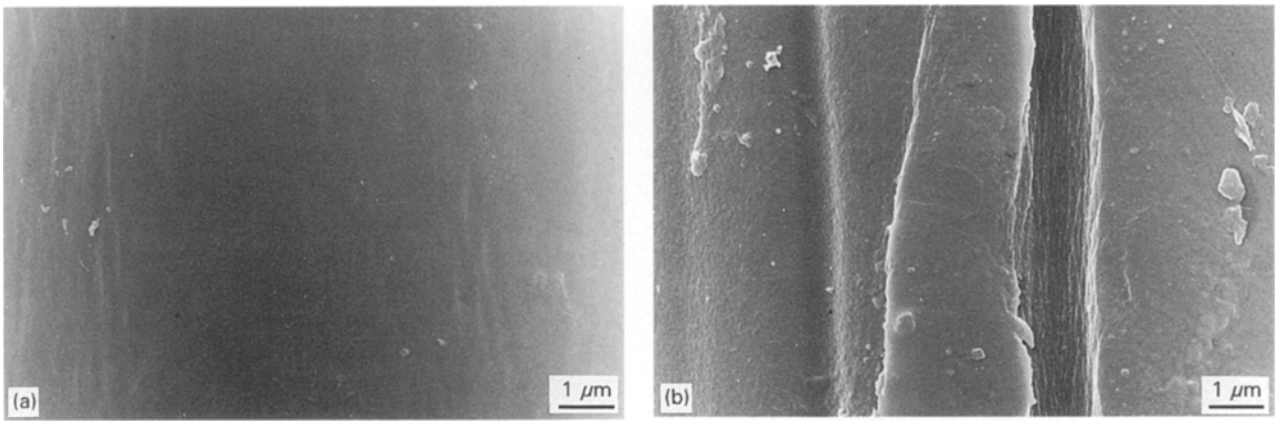

Figure 4 (a) PI-1 and (b,c) PI-4 fibre surfaces after permanganic etching (agent II).

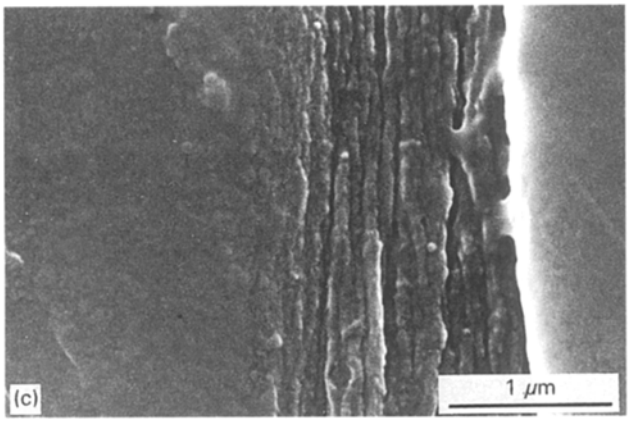

Figure 4 (continued).

iPP longitudinal sections with PI-4, Fig. 8e, and PI-2 fibres, Fig. 8f, clearly shows the difference in density of nuclei along the fibre surface.

At the interface between the iPP matrix and the PI-4 fibre, a large number of nuclei from which the transcrystalline zone grows have been observed. In Fig. 9a, b one can see several nuclei which consist of a sheaf of closely packed parallel lamellae 20 nm thick and of about 1 μm^2. At some places of the interface, the cross hatched lamellar morphology of iPP was observed very clearly, Fig. 9b, c. The bundles of stacked lamellae were inclined at some angle to the fibre axis, Fig. 10b, (notice that this micrograph was obtained with the sample tilted 30° to the plane of view). On the other hand, there are extended parts of

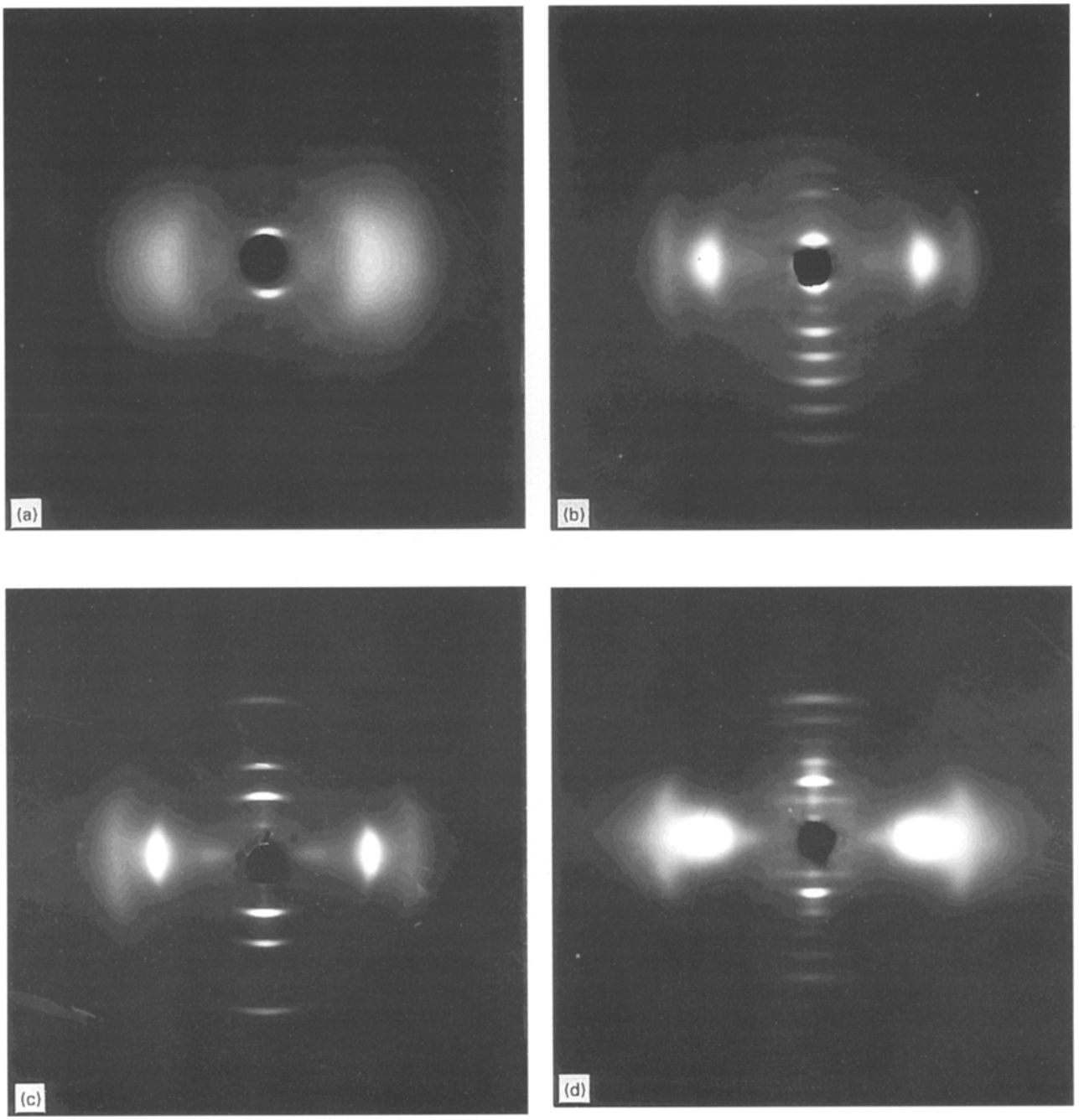

Figure 5 X-ray diffraction patterns of PI fibres: (a) PI-1, (b) PI-2, (c) PI-3 and (d) PI-4.

the interface with orthogonal orientation of lamellae to the direction of the fibre axis, Fig. 10a.

It is interesting that a similar beginning of melt growth of isotactic polystyrene (iPS, $M_w = 1.1 \times 10^6$ and $M_n = 3.8 \times 10^5$) was observed by Bassett [36]. On the etched cut surface of iPS, groups of lamellae, formed along the central thread, could often be seen. These lamellar groups existed in the unstressed and undeformed melt and therefore they could not be explained as a nucleation along flow lines resulting in "shish kebabs" [19]. An inherent entanglement associated with very long molecules was assumed to explain the nature of this phenomenon.

The present results are sufficient to suggest a model of the structure of the fibre reinforced iPP composites, Fig. 11. Nucleation inactive fibres PI-1 do not induce transcrystallization; nucleation occurs within the matrix and rarely on the fibre surfaces, Fig. 11a. Lamellae of grown spherulites follow round the fibre surface.

The very active fibre PI-4 favours nucleation on the fibre surface, and a large number of stacked lamellar structures arise at the interface, Fig. 11b. An isolated nucleus consisting of a sheaf of parallel needleshaped lamellae of uniform thickness of about 20–21 nm can be distinguished on the interface. The transcrystalline zone begins to grow from those nuclei. In the electron micrographs, the crosshatched lamellar morphology of the iPP interface has clear appearance. Such a peculiar habit of the crystalline growth is typical of the interfacial zone adjacent to the fibre surface, about 1–2 μm thick. Far away from the fibre surface, the transcrystalline zone has a morphology identical to that of the iPP matrix. This type of morphology is inherent to the centre of monoclinic iPP α spherulites [36].

Such a crosshatched interface morphology suggests epitaxial crystallization of the iPP matrix on the extended chain PI domains. These domains with extended parallel chains and a high degree of chain orientation exhibit smooth (on the molecular scale) surface fragments which favour the epitaxial folded chain iPP lamellar overgrowth. As the domains are

TABLE I Unit cell dimensions (nm) of polymers used

Polymer	*a*	*b*	*c*	Angles	Reference
iPP	0.665	2.096	0.650	$\beta = 99.3°$	[27]
PI-1	0.630	0.397	3.200	$\alpha = \beta = \gamma = 90°$	[43]
PI-2	0.858	0.548	2.090	$\alpha = \beta = \gamma = 90°$	[44]
PI-3	0.918	0.530	3.386	$\alpha = \beta = \gamma = 90°$	[45]
PI-4	–	–	2.452	–	–

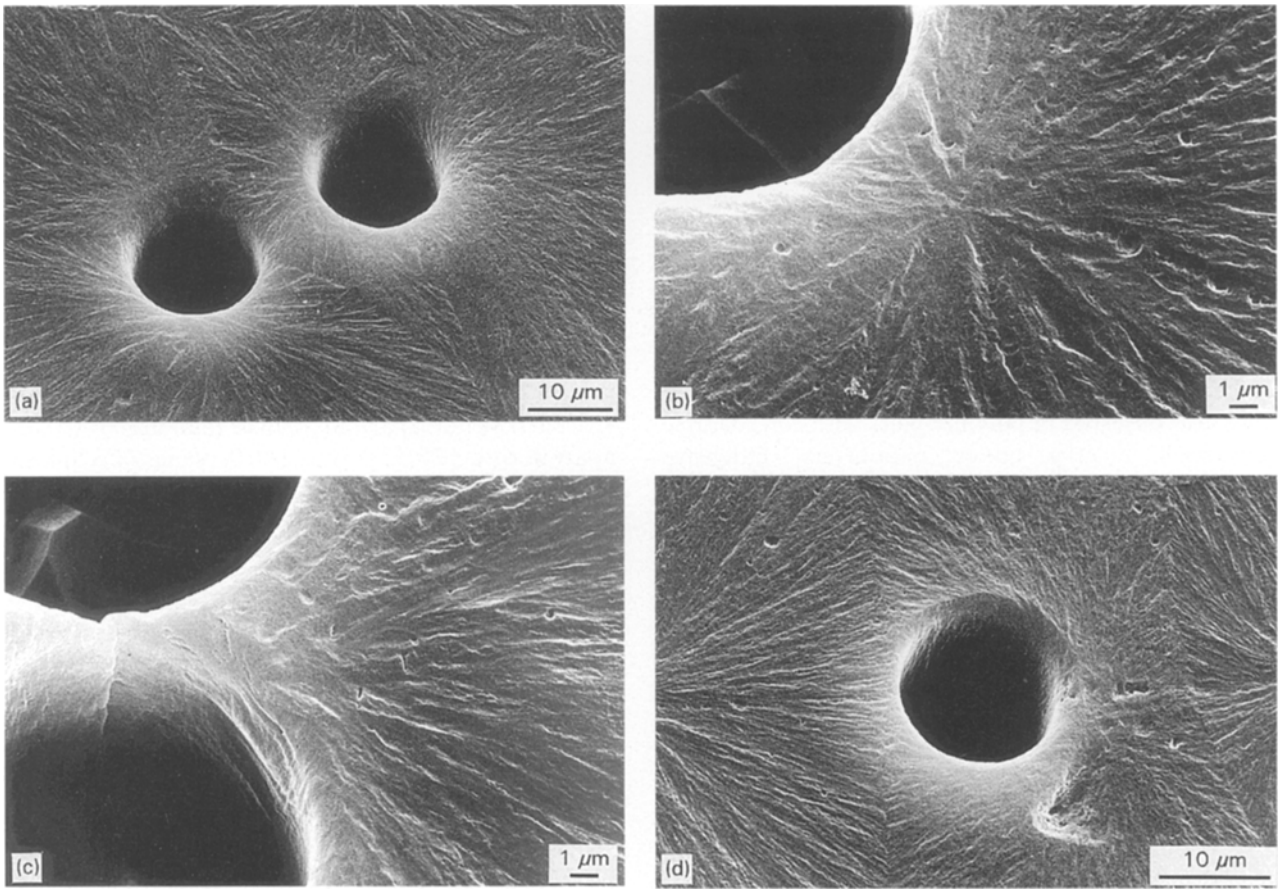

Figure 6 SEM micrographs of etched transverse (a–d) and longitudinal (e,f) sections of the iPP composite with PI-1 fibres. Black holes result from etched-off mesomorphic PI-1 fibres (the samples were tilted under a 30° angle).

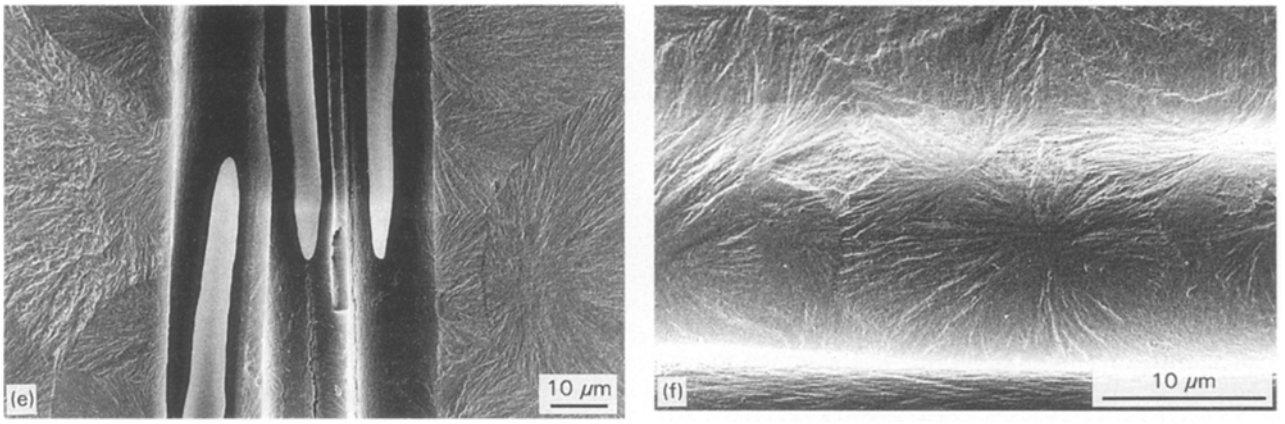

Figure 6 (continued).

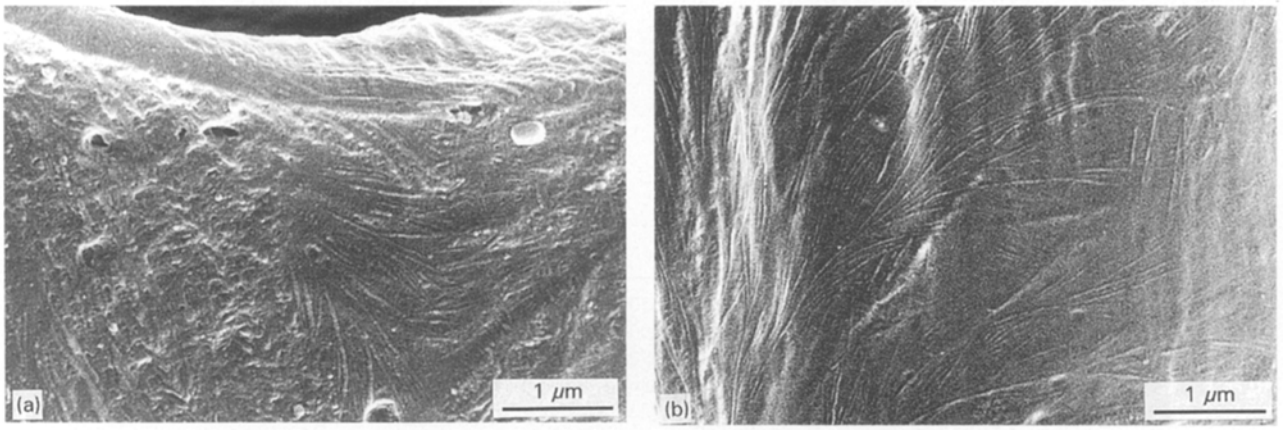

Figure 7 SEM micrographs of the etched iPP interface (PI-1 fibre removed): (a) transverse section and (b) longitudinal section.

slightly disorientated relative to each other, the nuclei are also slightly disorientated, as can be seen in Fig. 9a, b.

Epitaxy at the substrate's surface as a major factor in the nucleation process was investigated by Turnbull and Vonnegut [33] and Hobbs [34]. In their studies the pronounced nucleation effect observed with high modulus carbon fibres in iPP was explained by epitaxial growth of the matrix on large graphite planes present on the fibre surface. However, several authors [46, 47] suppose that epitaxy cannot be a generally valid explanation of transcrystallization, because it was also observed in polymer pairs with considerable mismatch in the lattice parameters. Extensive investigations of transcrystallization showed that these phenomena do not depend on the crystallographic parameters of the substrate [8, 24–27]. Though the criterion of lattice matching is considered to be very important for any epitaxial growth, there are some examples of epitaxial crystallization where the crystalline structures of polymer pairs are significantly different [48, 49]. Moreover, the presence of a wettable surface alone, without further orientation influence, can cause epitaxy in crystallizing macromolecules [50].

Transcrystallization was observed in iPP–natural cellulose fibre composition [10, 51], whereas the regenerated and mercerized cellulose fibres [10] and surface treated cellulose fibres [51] do not induce transcrystallization. The crystal structures of natural cellulose (cellulose I: $a = 0.82$ nm, $b = 1.03$ nm, $c = 0.79$ nm [51]) and iPP are appreciably different, and matching of crystal structure is not a ready explanation of transcrystallization. However, the occurrence of transcrystallization was explained by matching of the interchain distances between iPP and cellulose I chains [51]. On the (1 0 0) face of natural cellulose I, the distance between chains is 0.82 nm and the distance between the centres of adjacent glucose units along the chain is 0.515 nm. These spacings are similar to distances between the rows of methyl groups forming the "B" (0 1 0) face of iPP, which are spaced 0.84 nm apart in planes that are 0.505 nm apart in rows [27, 52]. Thus, (1 0 0) planes of cellulose I can initiate epitaxial iPP growth.

For the PI-2 fibre, the distance between polyimide chains on the (1 0 0) face is 0.858 nm and the distance between the centres of dianhydride moieties is 2.09 nm, as shown in Fig. 12. If the methyl groups of iPP chains are superimposed on the crystalline structure of PI-2 fibre, a very good agreement can be observed (methyl groups shaded). Hence, in this case the epitaxial overgrowth of iPP is able to induce nucleation. For the PI-4 fibre ($c = 2.45$ nm), epitaxy is also a possible explanation for the occurrence of transcrystallinity. In the case of the PI-3 fibre, matching of the interchain distances is not so good ($c = 3.386$ nm) as for PI-2 and PI-4.

The PI-1 fibres have a mesomorphic structure, with a degree of chain disordering about 60°. Epitaxial

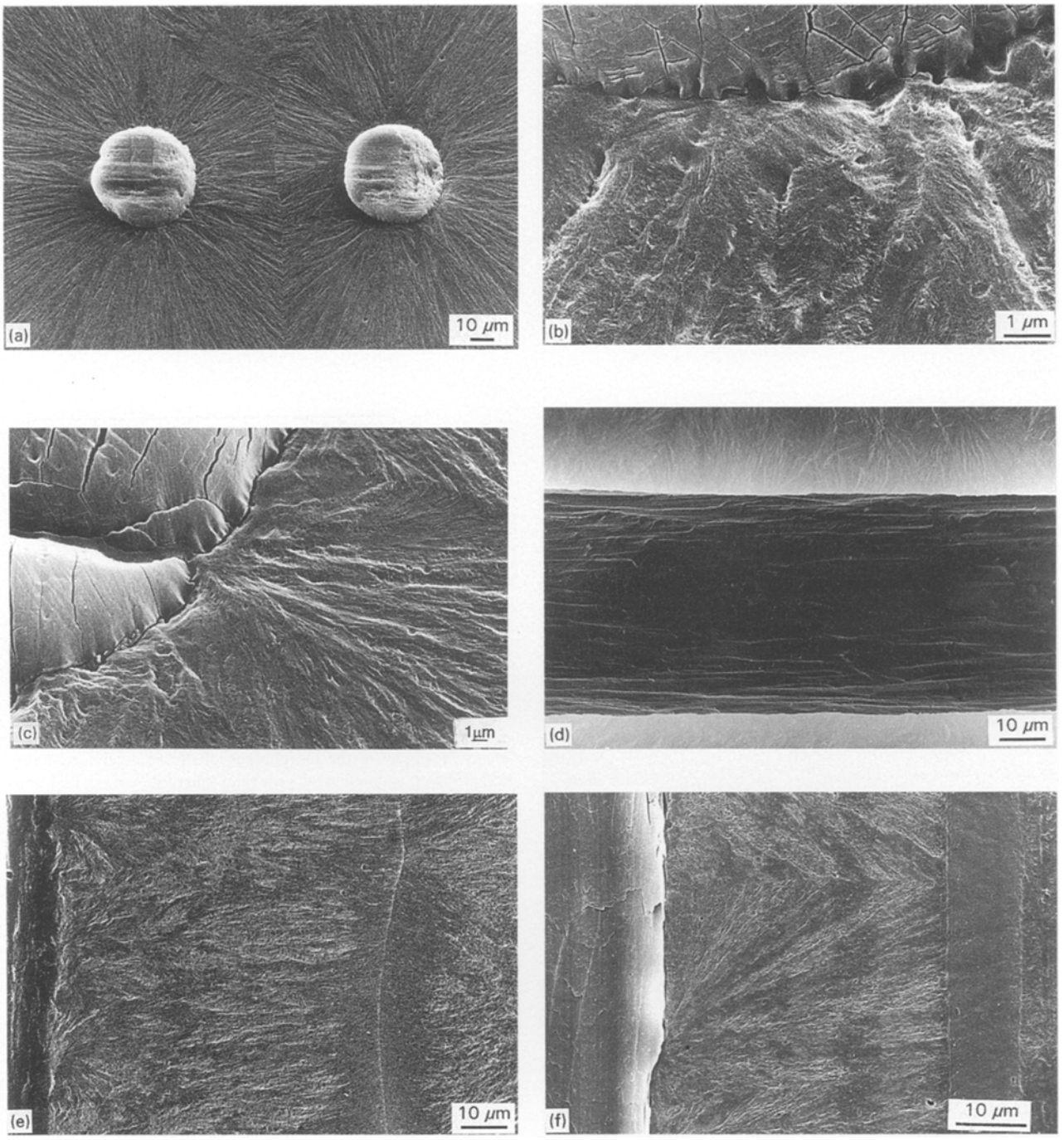

Figure 8 SEM micrographs of etched transverse (a–c) and longitudinal (d–f) sections of the iPP composite with PI-4 (a–e) and PI-2 (f) fibres (the samples were tilted under a 30° angle).

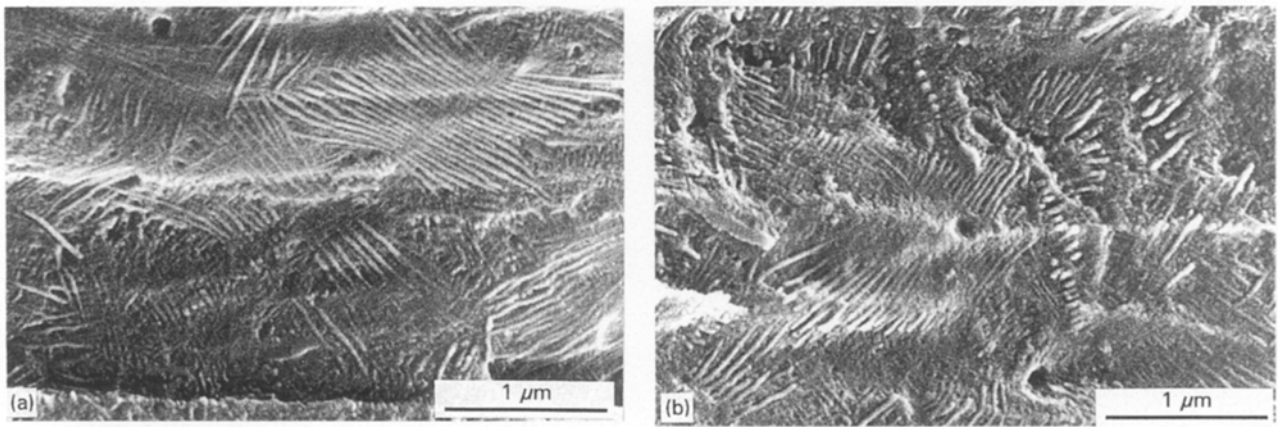

Figure 9 SEM micrographs of various parts of the etched iPP interface (PI-4 fibre removed, longitudinal sections): (a, b) the nuclei from which the transcrystalline zone grows, (c) the bundles of stacked parallel lamellae. The fibre axis is horizontal (tilt angle, 30°).

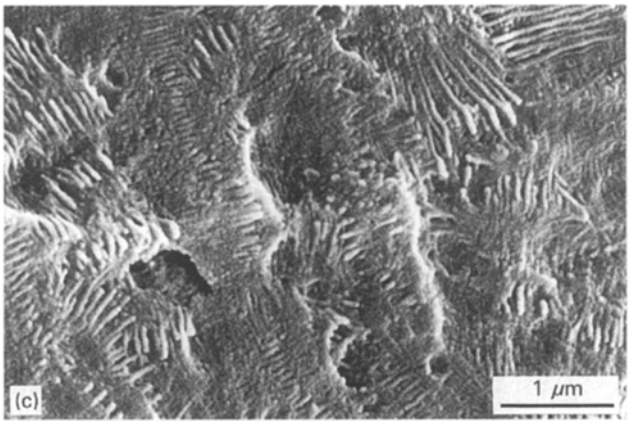

Figure 9 (Continued).

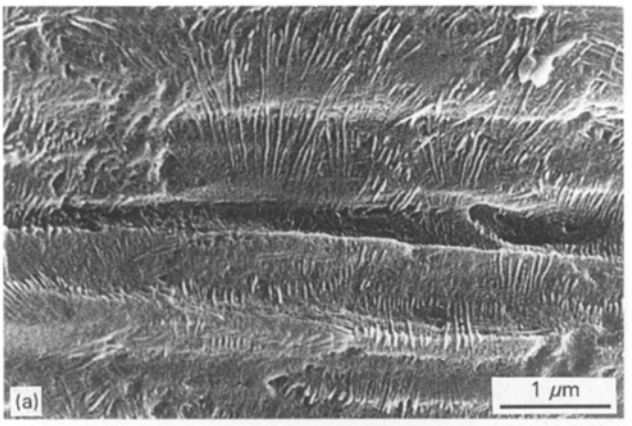

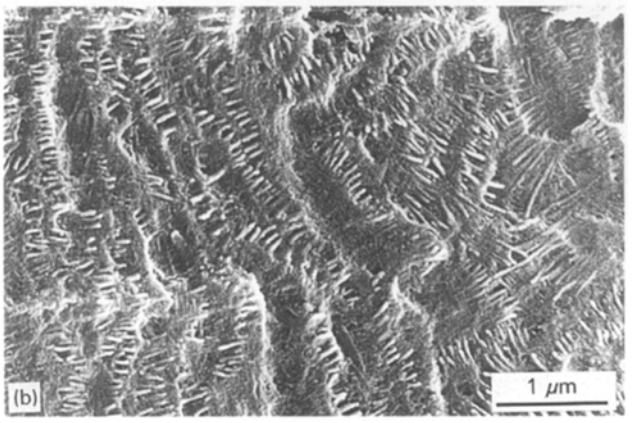

Figure 10 SEM micrograph of extended part of the iPP interface with orthogonal orientation of lamellae to the fibre axis (a) and the bundles of stacked lamellae under the angle to fibre axis (b) (tilt angle, 30°).

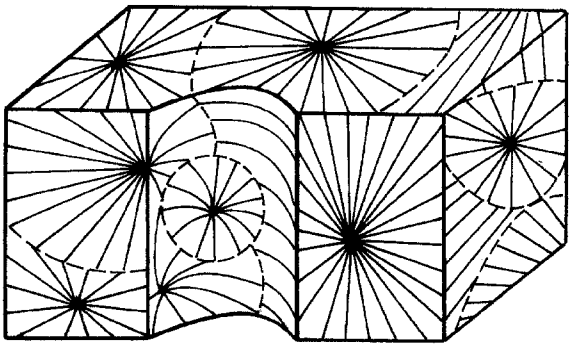

(a)

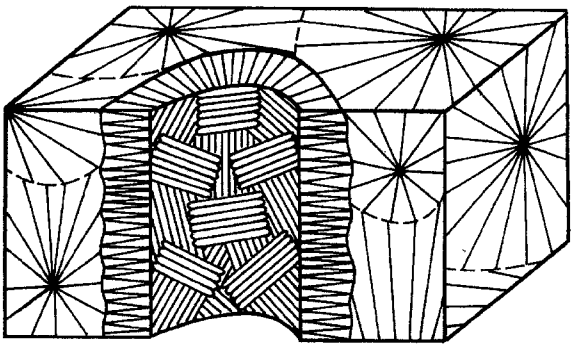

(b)

Figure 11 Model of the morphology of the fibre reinforced iPP composites: (a) non-epitaxial growth of spherulites on the PI-1 fibre surface, (b) epitaxial growth of the transcrystalline zone on the PI-4 fibre surface domains. Dimensions in the sketch are distorted (see the text).

overgrowth does not occur, and the interface and the bulk of iPP have the same spherulite morphology. On the other hand, PI-2, PI-3 and PI-4 fibres with domain structure (of extended parallel chains sufficiently long and with high degree of chain orientation) favour epitaxial growth, which induces transcrystallization.

Different densities of the transcrystalline interphase can be explained by the presence of disordered parts on the fibre surface, without nucleating sites. Therefore, the surface topography on the microlevel, seems to be the most essential parameter for the process of epitaxial iPP lamellae growth.

Gray [10] and Hobbs [53] also demonstrated that the topography of the substrate surface is a major factor in transcrystallization.

The nucleation activity of a substrate depends on the shape and the size of small parts of the surface ("shallow ditches") which could be large enough to accommodate a heterogeneous nucleus and to form stable lamella [34]. It was demonstrated that condensed aromatic compounds are very good nucleating agents for iPP [27, 34]. They consist of parallel layers or parallel rows of molecules which expose faces of hydrocarbon groups, while the polar groups are confined in the centre. As a result, the faces have shallow ditches of limited length in which adsorbed polymer molecules can be forced to assume a stretched conformation, making crystallization easier. In the present case, the PI fibres used have aromatic rings in their macromolecules. It is supposed that all of them are bound to be good nucleating agents. However, only the PI fibres, which exhibit regular packing of parallel stacks of the flat ring system, have a good nucleating ability and induce transcrystallization.

Differences in axial thermal expansion coefficients (TEC) between the fibres and the matrix were considered as a possible reason of transcrystallization [11, 12]. In this investigation the PI fibres studied

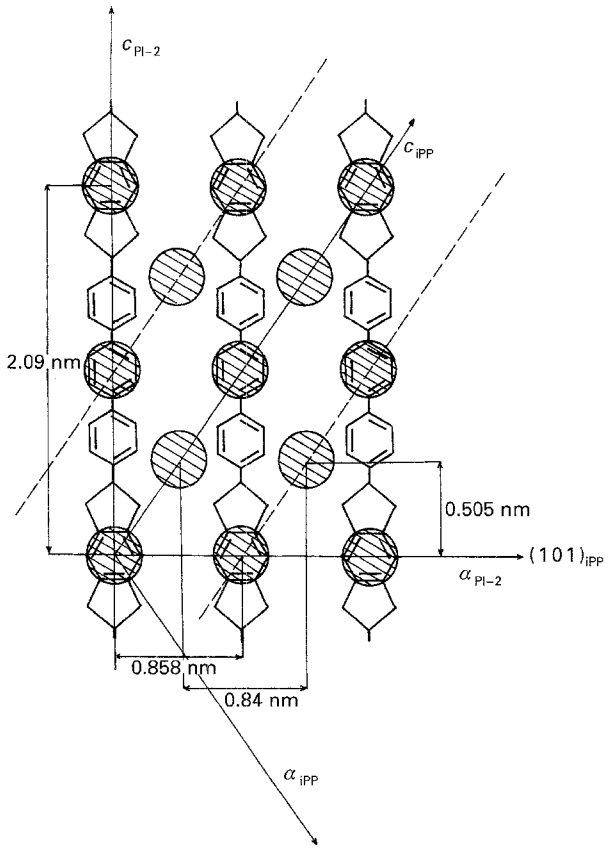

Figure 12 Matching of the interchain distances. The (1 0 0) face of the PI-2 fibre with "B" (0 1 0) face of iPP [52] superimposed (methyl groups shaded).

have similar TEC of the order $2 \times 10 \equiv {}^{5}\mathrm{K} \equiv {}^{1}$. The transcrystallization phenomenon cannot be explained by the big difference in TEC in this case. Explanations based on differences in TEC between nylon 66, poly(ethylene terephthalate) or polyester fibres and iPP matrix also do not seem to be valid, because TEC of these polymers are not vastly different [8]. Natural cellulose fibres induce transcrystallization, but regenerated and mercerized cellulose fibres [10] and treated cellulose fibres [51] do not induce transcrystallinity even though all these fibres have the same TEC.

4. Conclusions

Under the crystallization conditions applied, polyimide fibres were found to exhibit different nucleating abilities in the iPP matrix: PI-1 fibres were inactive, PI-2 and PI-3 moderately active, and PI-4 very active. That means that the occurrence of transcrystallization is dependent on the type of fibre used.

The surface induced transcrystalline interphase grows from nuclei which consist of a sheaf of closely packed needleshaped parallel lamellae of uniform thickness. The nuclei are linked in extended bundles.

The peculiar crystalline growth habit is typical of the interfacial zone adjacent to the fibre surface, about 1–2 μm thick, and has crosshatched lamellar morphology. At greater distances from the fibre surface, the transcrystalline zone has a morphology identical with that of the iPP matrix. Thus, the transcrystalline zone has a composed structure.

The chain folded lamellar overgrowth can be explained by epitaxial crystallization of the iPP matrix on the surface domains formed by extended parallel chains of PI fibres and by matching the fibre structure. The defective surface structure of fibres, observed in some of their parts, prevents the matching and decreases this nucleating ability.

Acknowledgements

The authors would like to express their acknowledgement to Dr J. Baldrian for valuable discussions, to Dr D. Hlavatá and Mrs M. Trnková for careful technical assistance. The work was supported by grant No. 203/94/0822 of the Grant Agency of the Czech Republic.

References

1. D. CAMPBELL and M. M. QAYYUM, *J. Mater. Sci.* **12** (1977) 2427.
2. M. AVELLA, E. MARTUSCELLI, C. SELLITI and E. GARAGNANI, *ibid.* **22** (1987) 3185.
3. M. J. FOLKES and S. T. HARDWICK, *ibid.* **25** (1990) 2598.
4. F. S. CHENG, J. L. KARDOS and T. L. TOLBERT, *SPE J.* **26** (1970) 62.
5. J. L. KARDOS, *J. Adhesion* **5** (1973) 119.
6. *Idem, Chemtech.* **14** (1984) 430.
7. R. H. BURTON and M. J. FOLKES, *Plast. Rubber Process. Appl.* **3** (1983) 129.
8. D. CAMPBELL and M. M. QAYYUM, *J. Polym. Sci., Polym. Phys. Ed.* **18** (1980) 83.
9. M. G. HUSON and W. S. McGILL, *ibid.* **23** (1985) 121.
10. D. G. GRAY, *J. Polym. Sci., Polym. Lett. Ed.* **12** (1974) 509.
11. J. L. THOMASON and A. A. VAN ROOYEN, *J. Mater. Sci.* **27** (1992) 889.
12. *Idem, ibid.* **27** (1992) 897.
13. E. JENCKEL, E. TEEGE and W. HINRICHS, *Kolloid Z.* **129** (1952) 19.
14. M. J. FOLKES and S. T. HARDWICK, *J. Mater. Sci. Lett.* **6** (1987) 656.
15. Y. G. LEE and R. S. PORTER, *Polym. Eng. Sci.* **26** (1986) 633.
16. S. Y. HOBBS, US Patent 3812077.
17. M. R. KANTZ and R. D. CORNELIUSSEN, *J. Polym. Sci., Polym. Lett. Ed.* **11** (1973) 279.
18. H. SCHONHORN, H. L. FRISH and G. L. GAINES, *Polym. Eng. Sci.* **17** (1977) 440.
19. M. J. FOLKES, S. T. HARDWICK and W. K. WONG, in "Polymer Composites", Proceedings of the 28th Microsymposium on Macromolecules, Prague, July 1985, edited by B. Sedláček (W. de Gruyter, Berlin, 1986) p. 33.
20. M. J. FOLKES and W. K. WONG, *Polymer* **28** (1987) 1309.
21. T. BESSELL, D. HULL and J. B. SHORTALL, *Faraday Symp. Chem. Soc.* **7** (1972) 137.
22. M. MASOUKA, *Int. J. Adhesion Adhesives* **1** (1981) 256.
23. P. J. A. RITCHIE and B. W. CHERRY, 13th and 14th Conferences on Adhesion (City University, London, 1975–76) Ch. 15, p. 235.
24. A. M. CHATTERJEE and F. P. PRICE, *J. Polym. Sci., Polym. Phys. Ed.* **13** (1975) 2369.
25. *Idem, ibid.* **13** (1975) 2385.
26. *Idem, ibid.* **13** (1975) 2391.
27. J. C. WITTMANN and B. LOTZ, *Prog. Polym. Sci.* **15** (1990) 909.
28. E. DEVAUX and B. CHABERT, *Polym. Commun.* **31** (1990) 39.
29. *Idem, ibid.* **32** (1991) 464.
30. J. VARGA and J. KARGER-KOCSIS, *Compos. Sci. Technol.* **48** (1993) 191.

31. T. OONO, F. KUMAMARU, T. KAJIYAMA and M. TAKAYANAGI, *Rep. Prog. Polym. Phys. Jpn.* **24** (1981) 193.
32. B. S. HSIAO and E. J. H. CHEN, *Mater. Res. Soc. Symp. Proc.* **170** (1990) 117.
33. D. TURNBULL and B. VONNEGUT, *Ind. Eng. Chem.* **44** (1952) 1292.
34. S. Y. HOBBS, *Nature, Phys. Sci.* **234** (1971) 12.
35. M. I. BESSONOV, M. M. KOTON, V. V. KUDRYAVTSEV and L. A. LAIUS, "Polyimides: Thermally Stable Polymers" (Consultants Bureau, New York, 1987) Chs. 1 and 3.
36 D. C. BASSETT, in "Developments in Crystalline Polymers – 2", edited by D. C. Bassett (Elsevier Applied Science, London, 1988) p. 99.
37. E. G. LOVERING, *J. Polym. Sci.* **A**-2 (1970) 1697.
38. S. MATSUOKA, J. H. DAANE, H. E. BAIR and T. K. KWEI, *J. Polym. Sci. Polym. Lett. Ed.* **6** (1968) 87.
39. R. H. OLLEY and D. C. BASSETT, *Polymer* **23** (1982) 1707.
40. F. RYBNIKÁŘ, *J. Appl. Polym. Sci.* **30** (1985) 1949.
41. *Idem*, in "Morphology of Polymers", Proceedings of the 17th Europhysics Conference on Macromolecular Physics, Prague, July 1985, edited by B. Sedláček (W. de Gruyter, Berlin, 1986) p. 309.
42. F. RYBNIKÁŘ, *J. Macromol. Sci. Phys.* **B30** (1991) 201.
43. M. KOCHI, H. SHIMADA, H. KAMBE, *J. Polym. Sci., Polym. Phys. Ed.* **22** (1984) 1979.
44. Y. G. BAKLAGINA, I. S. MILEVSKAYA, N. V. EFANOVA, A. V. SIDOROVICH and V. A. ZUBKOV, *Vysokomolek. Soedin.* **A 18** (1976) 1235.
45. Y. G. BAKLAGINA, I. S. MILEVSKAYA, N. V. LUKASHEVA, A. V. SIDOROVICH, V. V. KUDRYAVTSEV, T. A. MARICHEVA, M. M. KOTON, *Dokl. Akad. Nauk SSSR* **239** (1987) 1397.
46. R. H. BURTON and M. J. FOLKES, in "Mechanical Properties of Reinforced Thermoplastics", edited by D. W. Clegg and A. A. Collyer (Elsevier Applied Science, London, 1986) p. 269.
47. F. L. BINSBERGEN, *J. Polym. Sci., Polym. Phys. Ed.* **11** (1973) 117.
48. R. M. GOHIL *ibid.* **23** (1985) 1713.
49. T. TAKASHI, M. IMAMURA and I. TSUJIMOTO, *J. Polym. Sci. Polym. Phys.* **8** (1970) 651.
50. B. WUNDERLICH, "Macromolecular Physics" (Academic Press, New York, 1973) Vol. 1, p. 281.
51. D. T. QUILLIN, D. F. CAULFIELD and J. A. KOUTSKY, *J. Appl. Polym. Sci.* **50** (1993) 1187.
52. B. LOTZ and J. C. WITTMAN, *J. Polym. Sci., Polym. Phys.* **B24** (1986) 1559.
53. S. Y. HOBBS, *Nature, Phys. Sci.* **239** (1972) 28.

Received 15 June
and accepted 31 October 1994